

Kyoji TAKASE<sup>1</sup>

## Abstract

The present paper considers a process of ductile fracture from a semi-microscopic point of view on the basis of flow-curve which is obtained specially for that purpose. This flow-curve is a tensile flow-curve for plane strain whose distinctive feature is in its final portion and its associated hydrostatic stress-component. Comparing this flow-curve with other two kinds of deformations of the same mode i.e. plane strain, and yet, of different hydrostatic stress-component, it was found that hydrostatic stress-component greatly affects the strain at which internal damage appears, viz. the higher the hydrostatic stress (pressure), the larger is this strain. This phenomenon is composed of two processes, i.e. improving the uniformity of 'the internal deformation-pattern' and increasing the critical local strain at which microcrack appears. Whether this microcrack can grow to a macroscopic fracture or not depends not only on the local stress-state thereafter, but also on 'the restraint of adjacent domains'.

## 1. Introduction

The process of fracturing of ductile metals by free deformation, such as in case of tensile test, may be divided into three stages:

- (I) Initiation of local contraction.  
Let us call this stage 'the external limit of cold working'.
- (II) Creation of microcracks in the material of contracted portion.  
Let us call this stage 'the internal limit of cold working'.
- (III) Growth and aggregation of microcracks to a complete fracture.

The strain of the stage (i), that is the commencement of unstable deformation of external form, can be obtained, in principle (apart from

---

1. Member of the Japan Institute of Metals and the Iron & Steel Institute of Japan; Technical Research Institute, NIPPON KOKAN K.K., Kawasaki-shi, Japan.

the practice to solve the problem), from the strain-hardening characteristic or the flow-curve of the material. But, unfortunately, ordinary existing flow-curve is not yet sufficient for this purpose.

As for the stage (ii), our knowledge is still more obscure. For example, in case of uniaxial tensile test, which is an ordinary means to obtain a flow-curve, the stage (ii) is very near to the stage (iii) and it is hardly possible to locate the stage (ii) in the flow-curve because of the uncertainty of flow-curve near the fracture.

Hereupon there arises keen need for a new flow-curve which covers a strain range sufficient for discussing the above problems. Thus we must begin the study with flow-curve. The materials used for our experiment are mild steels.<sup>2</sup>

## 2. The Flow-Curve

It is generally accepted on the empirical basis that the stress-strain relationship varies according to deformation-mode, anisotropy, hydrostatic component of applied stress, etc.

In the present state of knowledge, the effects of above parameters are not so clear. Therefore we need many flow-curves for one material. Accordingly, the problem arises as to which arrangement of flow-curves is the most convenient to describe the plastic property of a material, in other words which parameters are to be adopted for flow-curve.

It may be natural to adopt the deformation-mode as the first parameter, and hydrostatic stress-component as the second parameter (the effect of anisotropy is automatically included in deformation-mode), considering Bridgman's (1) experiments under hydrostatic pressure.

### 2.1 Constant deformation-mode

The deformation-mode is defined to be constant when the ratios and signs of the three principal strains are constant and their principal axes are invariant with respect to the material. According to this definition, deformations by torsion or by shear are not of the constant deformation-mode.

2. Mild steels and probably almost all steels have tensile yield-stresses different from compressive yield-stresses (at high strain region). In this respect, it is significant to deal with steels.

The condition of constant ratios and signs of principal strains has almost the same meaning as that of constant ratios and signs of deviatoric stress-components (considering Lévy-Mises equation and anisotropy). Therefore, all stress-states of the same deformation-mode are on a half-quasi-plane (if there exists no anisotropy, then this is half-plane) whose edge is CC- which is the axis of symmetry for principal stress-axes (Fig. 1). It must be emphasized that it is a 'half' - quasi - plane. The opposite production of this half-quasi-plane is never of the same deformation-mode. Only in case of plane strain, the opposite production is also of plane strain, but not of the same deformation-mode. The opposite production of uniaxial tensile deformation is of uniaxial compressive deformation which is equivalent to bi-equiaxial tensile deformation. These circumstances may well be recognized considering the plastic anisotropies induced by those deformations.

### 2.2 Effect of hydrostatic pressure.

The followings are Bridgman's conclusions for uniaxial tensile deformation by experiments under high pressure.

- i) The flow-stress<sup>3</sup> under high hydrostatic pressure increases linearly with increasing hydrostatic pressure. This effect is small for small strains, but becomes larger and larger with increasing strains.
- ii) The maximum tensile load<sup>4</sup> increases with hydrostatic pressure, but its corresponding strain i.e. the strain at the commencement of local contraction is almost independent of hydrostatic pressure, and also after the commencement of local contraction, the profil of locally contracted portion is almost independent of hydrostatic pressure.
- iii) The fracture-strain (in logarithmic strain) increases linearly<sup>5</sup> with increasing hydrostatic pressure.
- iv) Under the same uniaxial tensile deformation-mode, the flow-stress at atmospheric pressure is almost independent of the hydrostatic pressure of prestraining.
- v) Under the same uniaxial tensile deformation-mode, the extra strain to fracture on second pulling at atmospheric pressure increases with the hydrostatic pressure of first pulling.

1. In this case, it means uniaxial tensile stress excluding the hydrostatic pressure (not component). Therefore, it means the flow-stress expressed in equivalent stress.
2. It means uniaxial tensile load excluding the hydrostatic pressure.
3. According to Pugh and Green (2), this is not always linear.

Among the above conclusions, i), iv) relate to flow-stress, ii) to external limit of cold working, and iii), v) relate to internal limit of cold working.

In Fig. 1, conclusions i) and iv) are expressed in the current front of plastic yielding AA-. Namely, in the half-quasi-plane of uniaxial tensile deformation, independent of loading path, the material yields when the stress-state attains the line AA- whose inclination against CC- is little when the strain is small, but becomes larger with increasing strain.

It may be quite natural to infer that above statements hold for any deformation of constant mode. Then considering that CC- is the axis of hydrostatic stress-component, flow-curve can be determined uniquely, when the deformation-mode and hydrostatic stress-component are given.

### 2.3 Tensile flow-curve for plane strain

For easiness' sake of experiment, let us consider plane strain problem. In this case, several methods are available to obtain flow-curve. Among them the one due to Watts and Ford (3) may be the most precise ever published. But this may be somewhat inconvenient for the purpose of discussing fracture, because of the stress-state employed in it.

Thereupon we searched for a new flow-curve with tensile stress-component and yet available to sufficiently high strain state to discuss fracture. Thus we have developed a new flow-curve by utilizing Bridgman's conclusion iv) in 2.2.

The principle of its method of obtaining is shown in Fig. 2. It may be noteworthy that the preparatory compression and the subsequent tensile test are nearly of the same deformation-mode because of the shape of the compressed portion, when the strain of this portion is above a certain value. This is suited for the application of Bridgman's result. Thus we can obtain 'a tensile flow-curve for plane strain' which has in general the form as shown in Fig. 3.<sup>6</sup>

In the figure, A indicates the yield point (the double line represents co-existence of two states: one before yielding, another after yielding).

6. In this paper, we utilize consistently 'r' (reduction in thickness in plane strain deformation) as the measure of strain. This r can be converted to any other expression of strain through the expression of equivalent strain.

B is the general elongation point. C and D are the points placed for convenience (C is near B and D is near E). The curve is, in general, fairly straight between C and D. The slope of CD is almost independent of the kind of steel. E is the maximum point, in the proximity of which damaging of the material begins by the preparatory compression. A little before E, on the flanks of specimen, there start minute cracks which will cause premature break-down of the specimen (therefore, these minute cracks must be ground off here). At F, the specimen breaks down completely by the indentation of cylinders. This point does not appear in most mild steels of good quality.

The region E - F may be called 'the damaging part of flow-curve' which represent the internal limit of cold-working by preparatory compression. The rest of the flow-curve is 'the non-damaging part' which is to be determined mainly by the general elongation point, because of the invariability of CD's slope.

The hydrostatic stress-component associated with the damaging part is of primary importance according to Bridgman's conclusion iii) in 2.2. This hydrostatic component is almost unaffected by the geometrical configuration of preparatory compression (within a certain range), but is considerably affected by the lubricating condition between the cylinder and the specimen. A normal course of hydrostatic stress-component during the preparatory compression is shown by the curve C in Fig. 5 (Takase (4)).

### 2.4 General aspect of flow-curve.

Generalizing the results of 2.3 and combining this with the generalized conclusions of Bridgman's experiment (2.2), we obtain Fig. 4, which shows the general aspect of flow-curve for a definite constant deformation-mode. Some explanations must be given about Fig. 4 (the hydrostatic stress-component is designated hereafter by 'p' taking compression in positive sign):

i) Yield-point and the flow-stress in the neighborhood of yield-point are almost unaffected by p.

ii) General elongation point: The strain of this point is little affected by p, but the stress of this point increases with p.

iii) Straight part: The stress (corresponding to the same strain) increases with p, and the slope increases at the same ratio.

In other words, the relative strain-hardening rate  $d\bar{\sigma}/d\bar{\epsilon}/\bar{\sigma}$  is little affected by p, from the region including general elongation point to fairly high strain, say  $\Gamma = 60\%$  (see Fig. 6. Note:  $\bar{\epsilon} = 1$  corresponds to  $\Gamma = 58\%$ ). For very high strain region, however, such a relation may not hold, and the relative strain-hardening rate increases with p (Fig. 6).

iv) Damaging part shifts to higher strain with increasing p.

### 3. Internal Limit of Cold-Working

As mentioned in 1, we can conceive two categories of limit of cold-working, i.e. external limit and internal limit. The former can be obtained, in principle, from the non-damaging part of flow-curve, and as it is not directly connected to fracture, further discussion of this problem may not be necessary. But there remains several essential problems to be solved concerning the problem of fracture.

One of them is 'the restraint of adjacent domains'. With the initiation of unstable deformation, there may occur a change in strain-distribution. The restraint of adjacent domains is a general term given by the author to any circumstances which impede the change in strain-distribution, when otherwise the external limit of cold-working will arrive. As for examples of this factor, we can mention rigid face of tools, friction, strain-gradient, 'closed shape' (as in shrinking flange in deep-drawing), etc.

The internal limit of cold-working is not necessarily connected with the external limit. Under certain restraint of adjacent domains, the internal limit occurs without the external limit. This is the case when the material deforms between rigid tool surfaces. This kind of deformation is very convenient to the experiment of the internal limit, because final sudden rupture of the material can considerably be separated from the internal limit. One example of this case is the preparatory compression of the flow-curve of 2. This is plane compression by cylinders.

The experiment for discussing the internal limit on the basis of this flow-curve must be so chosen that the deformation-mode and the restraint of adjacent domains are respectively same as that of the flow-curve, to avoid the confusion in argument. Thus we have chosen two kinds of deformation for comparative experiment, i.e. rolling of strip and ironing of cylindrical shell. These deformations are both of plane strain and are accomplished between rigid tool surfaces, consequently under the same restraint of adjacent domains.

#### 3.1 Experiment of plane strain

As already been described in 2.3, by plane compression between cylinders, internal damage of material begins near the strain of B, but by rolling of strip, internal damage of material cannot be observed even at strains far higher than those of B - F, except on edges of strip where small cracks are observed near the strain of F. By ironing of cylindrical shell, the strain just prior to the fracture by ironing with reduction-schedule composed of pass-reductions near theoretical maximum ( $\bar{\epsilon} \doteq 63.2\%$ ), falls in the vicinity of the strain of B, when the pass-reduction at the moment of fracture is fairly below the theoretical maximum (one single pass

has a certain range of pass-reduction because of the taper of mandrel), and by reduction-schedule composed of moderate pass-reduction, say  $\bar{\epsilon} = 30\%$ , internal damage appears without rupture of the draw-piece when the total strain has attained near the strain of B.

The difference between above three deformations can be clarified more effectively by microstructures. For example, in mild steel of ferrite-pearlite-structure (photo 1), pearlites deform evenly by rolling (photo 2) except at the edges of strip where pearlites deform with local contractions often accompanied by microcracks (photo 3). By compression between cylinders and ironing, the circumstances are the same (photo 4, 5, 6) as in the edge of rolled material.

These distribution-state of internal deformation may be termed 'the internal deformation-pattern'.

#### 3.2 Interpretation of the results

Since the above three deformations are of the same deformation-mode, there is no difference in deviatoric stress-components, and the difference is only in hydrostatic component. As for the restraint of adjacent domains, there is no difference as already been mentioned. The effect of strain-gradient due to the configuration of tools may be negligible for the minute domains like the extent of a pearlite grain.

Therefore, the above difference of internal deformation may be considered to be caused mainly by difference of hydrostatic stress-component. From this point of view, the above phenomena will be interpreted as follows.

The hydrostatic stress-components are:

(i) Plane compression by cylinders (Takase (4)):

$$p = 0.0 \bar{\sigma} \sim 0.2 \bar{\sigma}$$

in the strain-region where the damage of material can be seen. The coefficient of friction between the specimen and cylinders is assumed to be  $\mu \doteq 0.1$ .  $\bar{\sigma}$ , the yield-stress expressed in equivalent stress, is adopted as the unit of  $p$ , and positive sign means compression. The  $p$  in course of compression is shown by curve C in Fig. 5.

(ii) Rolling of strip:

$$p = \left( \frac{1}{\sqrt{3}} + \alpha \right) \bar{\sigma} \quad \text{except at the edges,}$$

$$p \doteq 0 \quad \text{at the edges,}$$

where  $\alpha$  is due to the friction between rolls and specimen. The  $p$  in course of rolling is shown by curve  $R_1 R_2 \dots$  in Fig. 5.

## (iii) Ironing of cylindrical shell:

$$p = \left( \frac{1}{\sqrt{3}} + \beta \right) \bar{\sigma} \quad \text{at the entrance of die,}$$

$$p > -\frac{1}{\sqrt{3}} \bar{\sigma} \quad \text{at the exit of die,}$$

where  $\beta$  is due to the friction between the draw-piece and mandrel and the taper of mandrel. The  $p$  in course of ironing is shown by curve I<sub>1</sub> I<sub>2</sub> ..... in Fig. 5.

Curves S<sub>A</sub> and S<sub>B</sub> show the internal limit of cold-working of steels A and B respectively (steel A may be considered to be of bad quality, and steel B, of good quality).

Let us make the interpretation taking steel A as the example. Now the point E for steel A is E<sub>A</sub>. Curve R<sub>1</sub> R<sub>2</sub> ..... crosses curve S<sub>A</sub> at A<sub>7</sub> where steel A is to be damaged internally by rolling. The strain of A<sub>7</sub> is far higher than that of E<sub>A</sub>. Therefore, internal damage hardly occurs in rolling.

In ironing, when we take the theoretically maximum pass-reduction, curve S<sub>A</sub> crosses with curve I<sub>1</sub> at A<sub>1</sub>, but the draw-piece does not rupture at this point, and after some ironing, ruptures at FA<sub>1</sub>. The strain of FA<sub>1</sub> is not decisively below that of F<sub>1</sub> (= strain of the theoretically maximum pass-reduction that is somewhat higher than 63.2%). Therefore, the ironing experiment is continued on to the second pass (  $\frac{2}{3}$  I<sub>3</sub> )<sup>7</sup> in which the draw-piece ruptures at FA<sub>3</sub> whose strain is fairly below the strain of F<sub>3</sub> and is near the strain of E<sub>1</sub>.

When the pass-reductions are moderate as shown by the upper curves, internal damage does not appear until A<sub>4</sub> of the fourth pass which is very near to E, but the draw-piece does not rupture in the fourth pass and can be transferred to the fifth pass I<sub>5</sub>. In the upper part of I<sub>5</sub>, the microcracks which have appeared at A<sub>4</sub> can be healed and disappear, and then at A<sub>5</sub>, the microcracks reappear (mostly at the localities different from the formers). These circumstances were verified by observing that the direction of microcracks is always nearly 45° to the direction of ironing and to the direction of wall-reduction.

7. The pass-reduction at the beginning of the second pass is a little below the pass-reduction at the end of the first pass, because of the taper of mandrel.

Thus the phenomena of internal damage can be clearly explained as the effect of hydrostatic stress-component. Then by what reason  $p$  affects the local deformation of pearlite? This may partly be explained utilizing Bridgman's result (Fig. 6). The sample used in his experiment was tempered pearlite of SAE 1045 steel (this is somewhat different from ordinary pearlite, but the circumstances may be the same). In Fig. 6, the relative strain-hardening rate is affected by  $p$  when  $\bar{\epsilon} > 1$  (see 2.4, iii)). Thus the relative strain-hardening rate increases with  $p$  in high strain region. Therefore, the local deformation is impeded by  $p$ , accordingly the strain (measured by external dimensions) at which microcracks appear, increases with  $p$ . The above explanation is also favoured by Bridgman's conclusion (v) in 2.2. Here must be mentioned another concealed phenomenon, i.e. the critical amount of slip for the creation of a microcrack is also considered to increase with  $p$ . This may have been perceived in the explanation of ironing limit.

## 4 Conclusions

i) Fundamental parameters for specifying a flow-curve are deformation-mode and hydrostatic stress-component. The concept of 'constant deformation-mode' is very important for treating the problem in a definite form.

ii) Limit of cold-working can be classified into two categories, i.e. 'the external limit' and 'the internal limit'. The former is concerned with the unstable deformation of external form. The latter is concerned with the unstable deformation of internal structure and is connected directly to fracture.

iii) A new flow-curve is developed. This flow-curve is composed of two parts, i.e. non-damaging part and damaging part. The non-damaging part concerns with the external limit of cold-working and the damaging part concerns with the internal limit of cold-working.

iv) The internal limit of cold-working is composed of two processes. At first, there occurs locally concentrated deformation in the internal structure and then, microcracks appear at localities of concentrated deformation. The distribution state of local deformation is termed 'the internal deformation-pattern'.

v) The internal limit of cold-working is greatly affected by hydrostatic stress-component. The internal deformation-pattern becomes uniform, and the critical local strain for the creation of microcrack becomes larger with increasing hydrostatic compressive stress-component. Thus the internal limit of cold-working can be much improved by high hydrostatic pressure component of applied stress.

vi) The microcracks of internal limit of cold-working do not necessarily develop immediately to a macroscopic fracture. It depends on the stress-state thereafter and also on 'the restraint of adjacent domains'.

References

1. P.W. Bridgman, *Studies in Large Plastic Flow and Fracture*, McGraw-Hill, Chaps. 1, 2 and 17 (1953).
2. H. LI, D. Pugh & D. Green, M.E.R.L. Plasticity Report No. 128. East Kilbride, Glasgow: Mechanical Engineering Research Laboratory (1956).
3. A.B. Watts & H. Ford, *Proc. Inst. Mech. Engrs.* 1B, 448(1952-53); *ibid* 169(1955).
4. K. Takase, *Nippon Kokan Technical Report No.3*, 1 (1964).

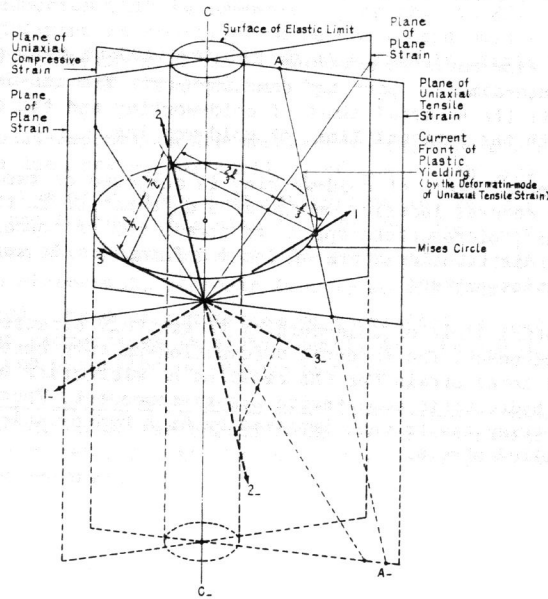


Fig. 1 Stress-space and deformation-mode

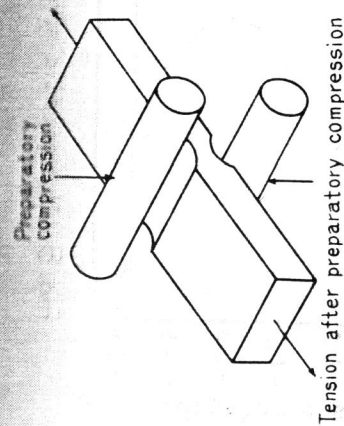


Fig. 2 Principle of obtaining the tensile flow-curve for plane strain

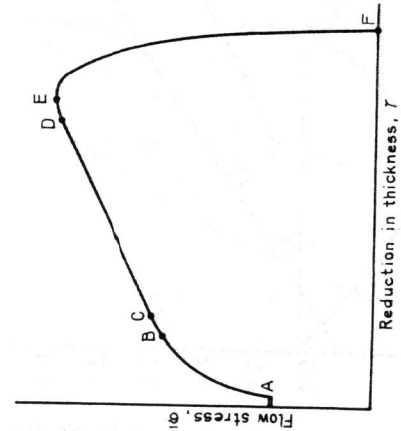
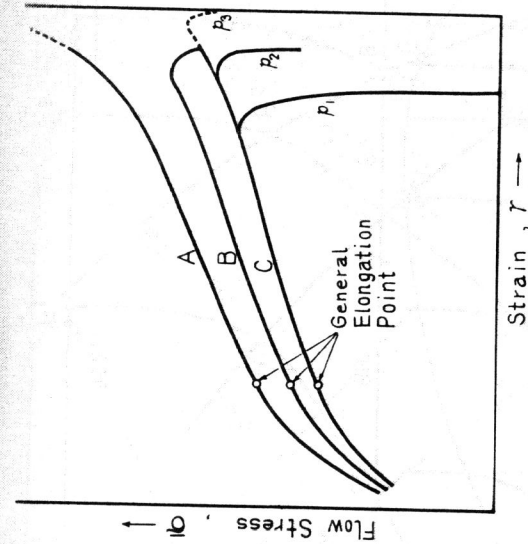


Fig. 3 Schematic representation of the flow-curve obtained by the principle of Fig. 2



Curve A: At sufficiently high pressure ( $p_3$ ),  
 Curve B: At moderately high pressure ( $p_2$ ),  
 Curve C: At atmospheric pressure after pre-straining at pressure  $p_1, p_2$  or  $p_3$ .  
 $p_1 < p_2 < p_3$

Fig. 4 Effect of hydrostatic pressure upon flow-curve

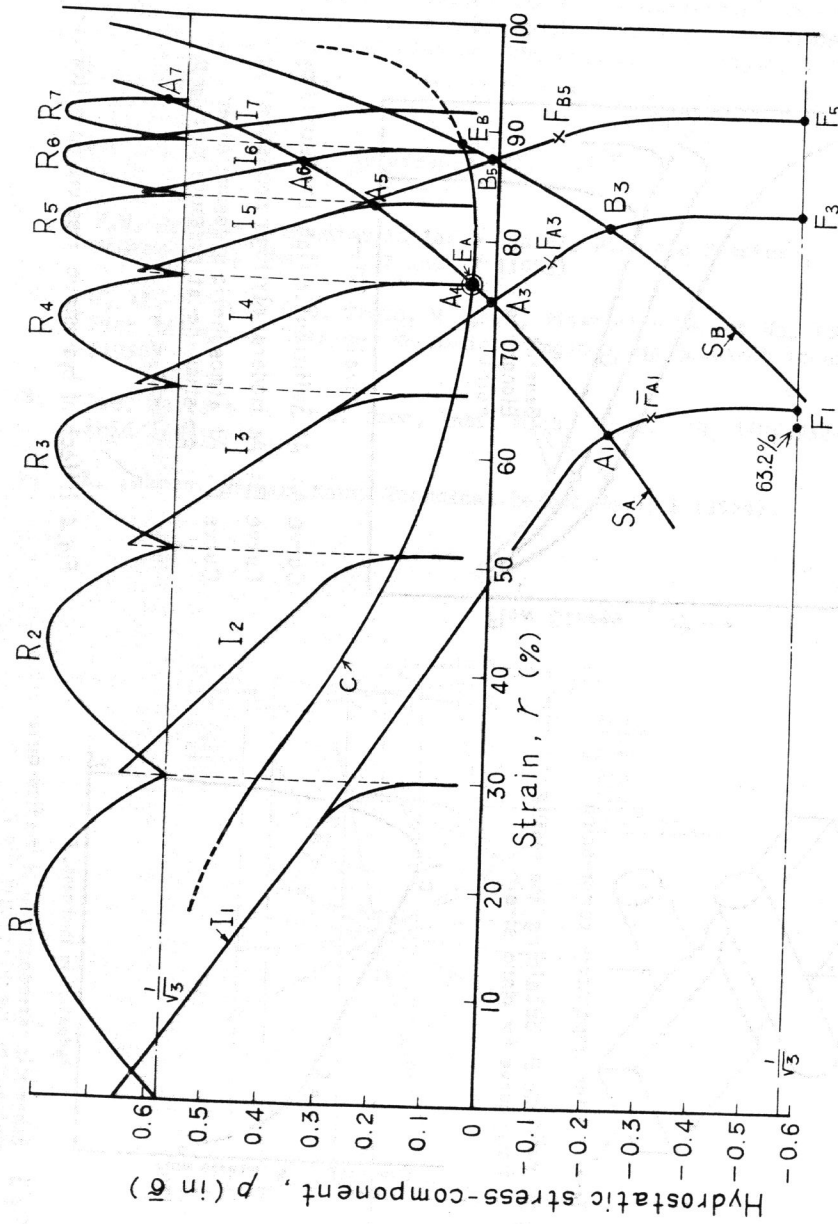


Fig. 5 Hydrostatic stress-component in various deformations of plane strain

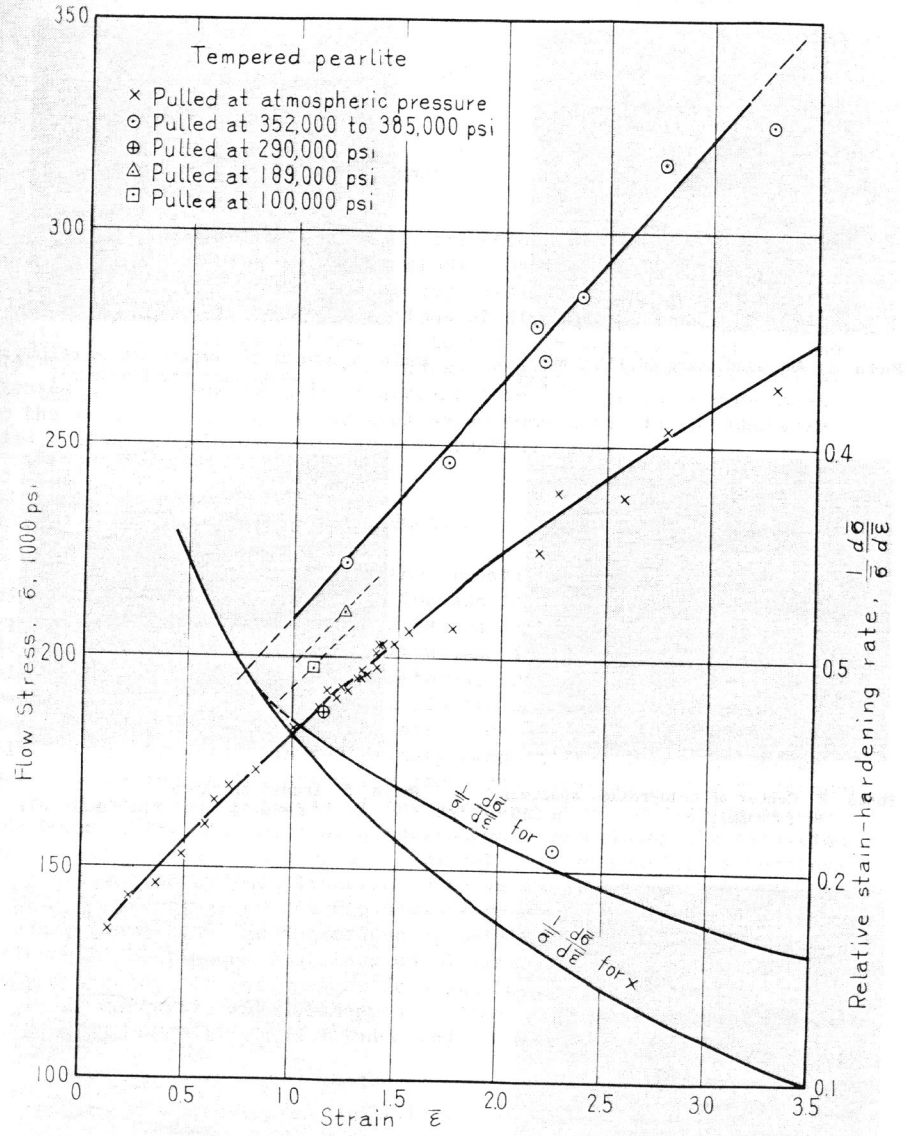


Fig. 6 Effect of hydrostatic pressure upon flow stress (by BRIDGMAN) and upon relative strain-hardening rate (supplemented by TAKASE)

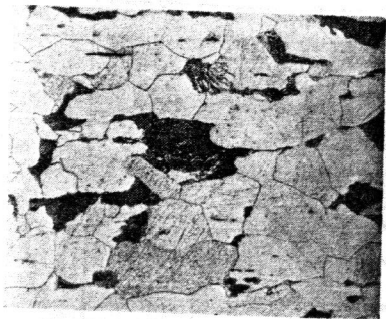


Photo 1 Annealed state (0.15% C steel),  
x 250

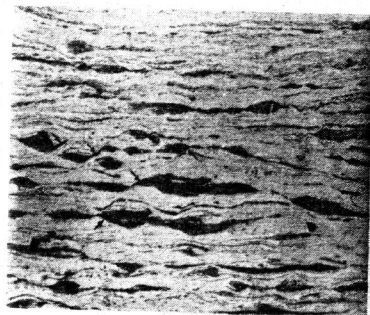


Photo 4 Center of compression by cylinders  
( $\Gamma=84\%$ , near the fracture),  
x 250

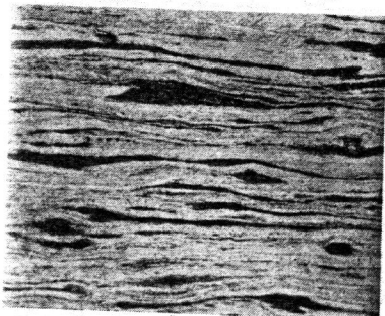


Photo 2 Center of cold-rolled specimen  
( $\Gamma=85\%$ ), x 250

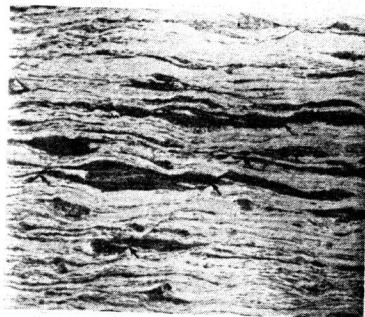


Photo 5 Ironed specimen  
( $\Gamma=86.5\%$ , near the fracture),  
x 250

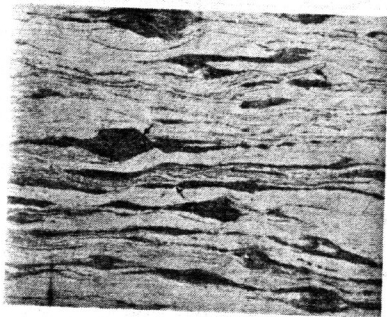


Photo 3 Edge of cold-rolled specimen  
( $\Gamma=85\%$ ), x250.  
Arrows indicate microcracks

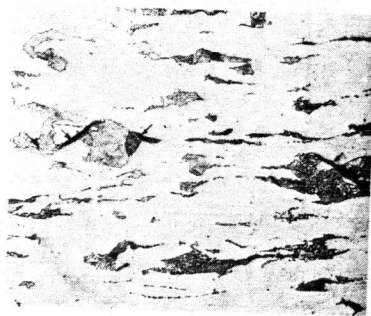


Photo 6 Ironed specimen  
( $\Gamma=63\%$ , maximum pass-reduction),  
x 250